

# We are IntechOpen, the world's leading publisher of Open Access books Built by scientists, for scientists

6,900

Open access books available

186,000

International authors and editors

200M

Downloads

Our authors are among the

154

Countries delivered to

TOP 1%

most cited scientists

12.2%

Contributors from top 500 universities



WEB OF SCIENCE™

Selection of our books indexed in the Book Citation Index  
in Web of Science™ Core Collection (BKCI)

Interested in publishing with us?  
Contact [book.department@intechopen.com](mailto:book.department@intechopen.com)

Numbers displayed above are based on latest data collected.  
For more information visit [www.intechopen.com](http://www.intechopen.com)



---

# Hot Filament Chemical Vapor Deposition: Enabling the Scalable Synthesis of Bilayer Graphene and Other Carbon Materials

---

Frank Mendoza, Tej B. Limbu, Brad R. Weiner and Gerardo Morell

Additional information is available at the end of the chapter

<http://dx.doi.org/10.5772/63921>

---

## Abstract

The hot filament chemical vapor deposition (HFCVD) technique is limited only by the size of the reactor and lends itself to be incorporated into continuous roll-to-roll industrial fabrication processes. We discuss the HFCVD reactor design and the interplay between the reactor parameters, such as filament and substrate temperatures, filament-to-substrate distance, and total pressure. Special attention is given to the large-area synthesis of bilayer graphene on copper, which is successfully grown by HFCVD with transmittance greater than 90% in the visible region and no gaps. We also discuss the HFCVD synthesis of carbon nanotubes, microcrystalline diamond, and nanocrystalline diamond.

**Keywords:** hot filament chemical vapor deposition, bilayer graphene, diamond, carbon nanotubes, 2D material

---

## 1. Introduction

Graphene can be obtained by a variety of techniques, including mechanical and chemical exfoliation of graphite, and chemical vapor deposition (CVD) methods, such as hot wall and hot filament CVD. Each technique has its own advantages and disadvantages that have to be weighed according to the intended application. The mechanical exfoliation of graphite produces high-quality monolayer graphene flakes [1, 2], whereas chemical exfoliation produces graphene flakes with significant structural defects [3]. Although the individual micron-scale

graphene flakes can be used to make miniature test devices that provide useful insight into the physical properties and potential applications of graphene [3], the reality is that graphene powders obtained by exfoliation methods are not useful for the mass production of reliable and reproducible electronic devices. However, hot-wall CVD appears to be the most straightforward method to produce monolayer graphene films with low defect density, typically on Cu substrates [4]. Nonetheless, the graphene films obtained by this technique are polycrystalline and discontinuous [5]. **Table 1** compares the physical properties of graphene obtained by different methods.

Method	Crystallite size ( $\mu\text{m}$ )	Sample size (mm)	Charge carrier mobility (room temperature) ( $\text{cm}^2\text{V}^{-1}\text{s}^{-1}$ )	Sheet resistance ( $\Omega/\text{sqr}$ ) / 2L
Mechanical exfoliation [1, 2]	~1 [5]	~1 [8]	(2L) $>10^4$ (at low temperature) [9]	$10^2$ [9]
Chemical exfoliation [3]	$\leq 0.1$ [3]	Large area of overlapping flakes [3]	100 (for a layer of overlapping flakes) [5]	30 k $\Omega$ Drop-cast film [3]
Chemical exfoliation through graphene oxide [3]	~100 [3]	Large area of overlapping flakes [3]	200–300 (for a layer of overlapping flakes) [8]	8–150 k $\Omega$ Multilayer Langmuir-Blodgett film [3]
CVD [9]	0.5 [5]	~5 [10]	5000 [9]	900 [11]
Epitaxial growth (SiC) [12, 13]	50 [5]	50 [5]	15,000 [14]	150–300 [15]
HFCVD [7]	$\leq 0.1$ [7] 0.1–0.2 [16]	30 [7]	~2500 [This work]	~800 [This work] ~650 [16]

**Table 1.** Properties of graphene films obtained by different methods.

An alternative approach to advance the potential applications of graphene is to focus the attention on bilayer graphene, which has a zero band gap like monolayer graphene. Furthermore, the band gap of bilayer graphene has been shown to be tunable, and its domain walls have shown ballistic electron-conducting channels [6]. These exciting physical properties expand the potential applications of bilayer graphene beyond those of monolayer graphenes.

Mendoza et al. [7] reported that large-area bilayer graphene can be grown by hot filament chemical vapor deposition (HFCVD) with transmittance greater than 90% in the visible region and no gaps. The size of the graphene wafers that can be obtained by HFCVD is only limited by the size of the reactor and lends itself to be incorporated into a continuous roll-to-roll fabrication process, thus lowering the cost per unit area and enabling the integration of bilayer

graphene in large-scale industrial production lines. The HFCVD method has the potential to enable large-area applications of graphene, such as transparent electrodes for flat panel displays and solar cells. In this chapter, we review the HFCVD state of the art for the synthesis of bilayer graphene and provide insight into how to tune the synthesis process to obtain optimum bilayer graphene films. We also discuss the HFCVD synthesis of diamond and carbon nanotubes.

## 2. The hot filament chemical vapor deposition reactor

The hot filament chemical vapor deposition (HFCVD) technique relies on a heated coiled wire to decompose the precursor reactants present in the gas mixture and deposit a film on the substrate surface kept near the filament at lower temperatures. HFCVD was introduced in 1979 for the synthesis of amorphous silicon films from silane gas at low substrate temperatures and high deposition rate [17]. For the synthesis of carbon materials (e.g., diamond, carbon nanotubes, graphene), a gas mixture consisting of a hydrocarbon (e.g., methane, acetylene) diluted in hydrogen is decomposed utilizing a refractory metal filament (such as tungsten, tantalum, or rhenium) that is resistively heated and maintained to 1800–2300°C, as measured with a dual wavelength pyrometer. Heterogeneous reactions at the hot filament surface and the emissive properties of the incandescent filament [18–21] initiate the decomposition of the hydrocarbon gases and the subsequent cascade of chemical vapor reactions. The filament temperature plays an essential role and influences the type and quality of the carbon materials that are grown. For example, at filament temperatures below 1800°C, little or no diamond film is obtained. Higher filament temperatures up to 2300°C lead to higher growth rates and higher quality polycrystalline diamonds. However, the higher the filament temperature, the faster the filaments become carburized. The metal carbides are brittle, resulting in relatively short

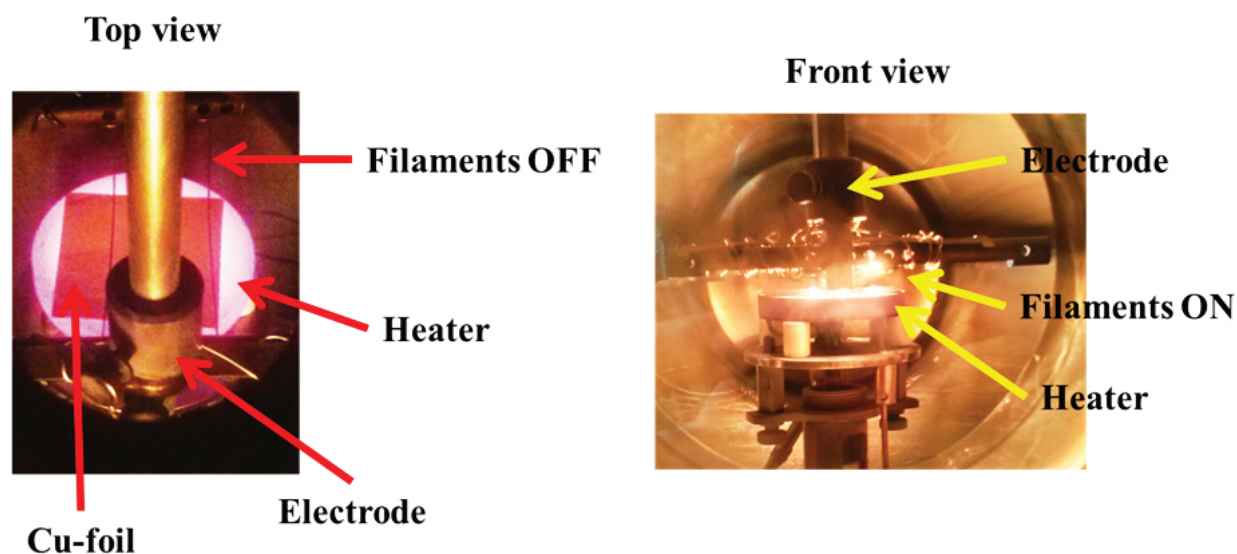


**Figure 1.** Internal details of the HFCVD setup for large-area graphene film deposition.

filament lifetimes and unsteady growth conditions. For stability and reproducibility, the filament material of choice is rhenium, which carburizes very slowly and lasts many cycles before requiring replacement.

For a 5-cm wafer, the HFCVD reactor typically consists of a 20-liter six-way cross stainless steel chamber. The substrate holder sits on the top of the substrate heater at the center of the chamber. The filament assembly is kept 5–10 mm above the substrate holder. **Figure 1** shows an actual picture of the main internal components in an HFCVD system. The filament wire diameter, length, and geometry must be optimized according to the intended film size, as well as the filament temperature and gas pressure required by the specific chemical vapor deposition reaction. It is necessary to assess the filament material's resistivity as a function of temperature and pressure. For example, the empirical resistivity of rhenium is approximately  $2 \times 10^{-6} \Omega \cdot \text{m}$  at  $2000^\circ\text{C}$  and  $3 \times 10^3 \text{ Pa}$ . The filament is held fixed by two parallel electrodes made of a refractory metal, typically molybdenum, to avoid evaporation of the electrode material onto the growing film. Coil-shaped filaments are often used because they enhance the total surface area available for initiating the heterogeneous decomposition reactions, but they tend to bend downward over time during film growth causing unsteady growth conditions. A filament arrangement consisting of multiple parallel stretched filaments of 0.25–0.50 mm diameter, as shown in **Figure 1**, is usually a better choice because it enhances the uniformity and total area of the resulting films while also providing considerable surface area for the heterogeneous decomposition reactions. However, the multiple filament arrangement requires very high-current power supplies.

The substrate temperature required for the synthesis of a particular material is determined by the residence time and mobility of reactant molecules and radicals that adsorb at the substrate surface. In the HFCVD reactor, the substrate temperature is intrinsically affected by the filament temperature and power, filament-to-substrate distance, and total pressure. Therefore, active substrate temperature control is needed in most cases in order to be able to optimize the quality of the films grown. While the filament temperature is dictated by the energy required to break the precursor gas molecules to initiate the chemical vapor reactions, the filament-to-substrate distance and total pressure are determined by the mean free path of critical radicals that form at or near the filament and must travel to the substrate surface before they get scavenged through other chemical reactions that do not lead to film deposition.

Besides determining the required filament and substrate temperatures, filament-to-substrate distance, and total pressure, the choice of substrate material and gas composition are also critical parameters to obtain the intended film type and quality. For example, under the same conditions, diamond can grow on molybdenum but not on quartz. The right gas-phase chemical environment and substrate temperature are conditions necessary but not sufficient to grow the intended film. The heterogeneous reactions that take place at the substrate surface are critically important in any chemical vapor deposition process. Therefore, the appropriate substrate must be provided to adsorb the reactive chemical species from the gas phase and catalyze the film synthesis reactions. After the right substrate is provided, the relative abundance of reactive chemical species will determine the film quality and growth rate and is primarily determined by gas composition. Priming or preparation of the substrate surface is

usually needed because it is covered with all sorts of adsorbates from the ambient environment; seeding may also be needed in some cases. The priming may be done before insertion in the HFCVD chamber or during the initial HFCVD process. For example, diamond growth on silicon must be preceded by diamond seeding prior to insertion in the HFCVD and by the removal of the native silicon oxide layer, which can be accomplished by attack of the hydrogen radicals in the HFCVD [Solid State Communications 116, 217, 2000]. In this case, there is an induction period during which the intended film does not grow until the substrate surface is ready to adsorb the reactive species. In the case of graphene grown on copper foil, the copper oxide layer is first removed by exposure to hydrogen at 1000°C.

### 3. Reports on HFCVD graphene

Singh et al. [16] reported the growth of large  $sp^2$  domain size (117–279 nm) single, bilayer, and multilayer graphene films on thick Ni foils using HFCVD at a relatively low substrate temperature of 700°C and low pressure (<200 Pa) at relatively short deposition time (10–30 min). The strategy used in this work is based on the mechanism by which hydrocarbon molecules decompose at the metal surface and diffuse into the bulk. Carbon diffuses into the bulk of nickel while it is kept hot and precipitates on the nickel surface forming nonuniform and discontinuous graphene layers during the fast cooling phase. This work presents the HFCVD as the advantage to dissociate at high temperature on filaments (tungsten filament at 1800–2200°C) source gases while temperature on heater is relatively low (700°C) compared with other CVD process obtaining high-quality films. Accordingly, with the different characterization (i.e., Raman spectra and SAED-TEM) presented in his report, the graphene samples (1–6 layers) obtained on nickel shows good crystallinity and also low sheet resistance values (630  $\Omega$ /sqr).

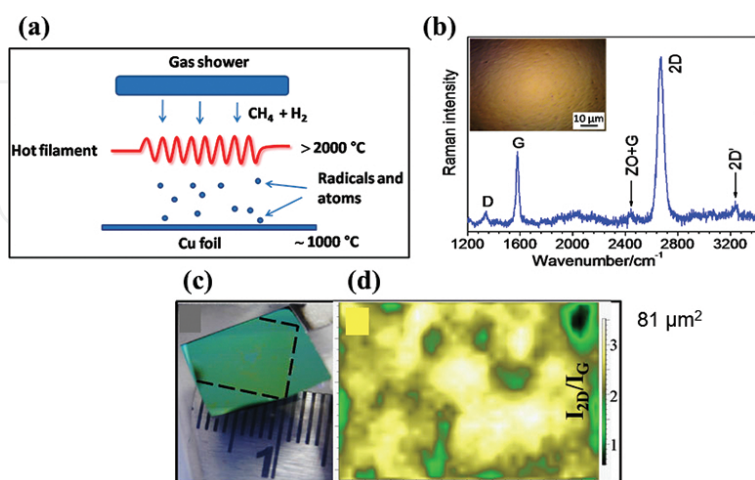


**Figure 2.** (a) Schematic diagram of the HFCVD used, (b) Raman spectra of the graphene obtained, (c) picture of the graphene transferred on  $SiO_2$  substrate, and (d) Raman mapping of a selected area of the hydrogenated graphene. (Image adapted with permission from Kataria et al. [22]).

Using Cu instead of Ni and higher substrate temperature, Kataria et al. [22] reported the growth of relatively large discontinuous patches ( $\sim 100 \mu\text{m}^2$ ) of high-quality monolayer graphene at  $1000^\circ\text{C}$  by HFCVD, see **Figure 2a** the schematic diagram about HFCVD used. This report is summarized in **Figure 2**. Through **Figure 2b**, we can see that the graphene obtained is monolayer, which is corroborated by Raman area map in **Figure 2c**. The Raman spectra in these samples showed an additional band termed 2D' peak ( $2946 \text{ cm}^{-1}$ ) in combination with D ( $\sim 1353 \text{ cm}^{-1}$ ) and G ( $1622 \text{ cm}^{-1}$ ) bands, indicating hydrogenated graphene. Kataria's group analyzed the possibility to remove hydrogen from the graphene samples by applying temperatures up to  $600^\circ\text{C}$  in inert atmosphere. These procedures and Raman spectroscopy examination confirm the desorption of hydrogen from the graphene samples.

Behura et al. [23] reported the synthesis of nonuniform large-domain graphene films on Cu substrates inside a HFCVD reactor [24, 25]. From the report, it is not clear that they actually used the filament during the synthesis process. The material obtained shows high number of defects in the film. This is observable through the large intensity of D-band accordingly with the Raman spectra. Also, the intensity ratio between the G and 2D bands is  $\sim 0.7$ , and the FWHM of the 2D band is  $\sim 55 \text{ cm}^{-1}$  indicating the growth of few-layer graphene. This report is summarized in **Figure 3**.

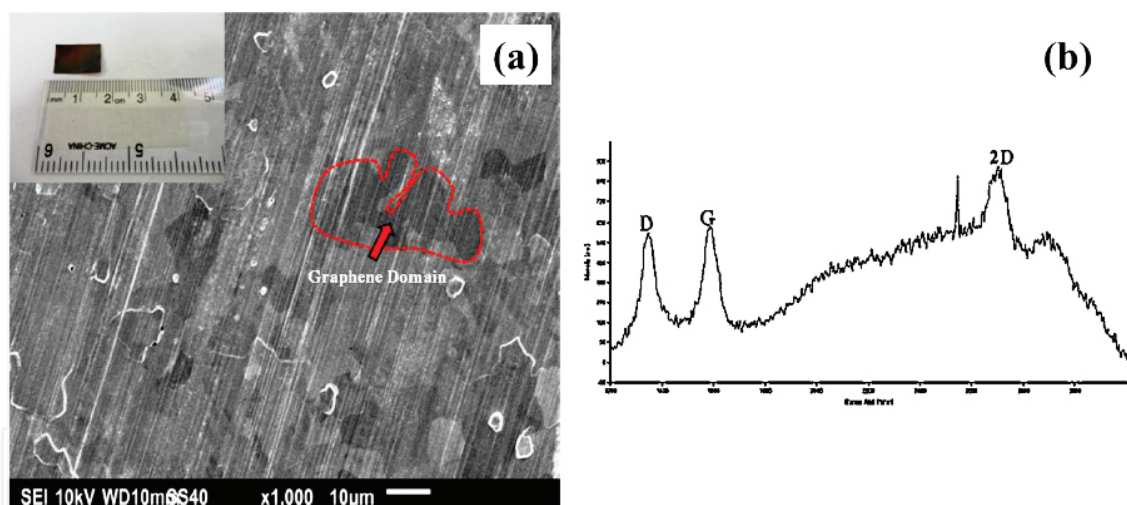


**Figure 3.** (a) SEM micrograph of graphene films on Cu surface with optical photograph shown in the inset, (b) Raman spectrum of graphene film on Cu surface. (Image adapted with permission from Behura et al. [23]).

#### 4. Obtaining uniform bilayer graphene by HFCVD

The general process to grow graphene by HFCVD is represented in **Figure 4**. The first step is the removal of the copper oxide layer from the copper substrate by exposure to hydrogen at  $1000^\circ\text{C}$ . We carry out this step at  $4.7 \times 10^3 \text{ Pa}$  for 30 min. The second step is the actual growth of graphene by adding methane to the gas mixture and heating the filament to  $1800^\circ\text{C}$ .

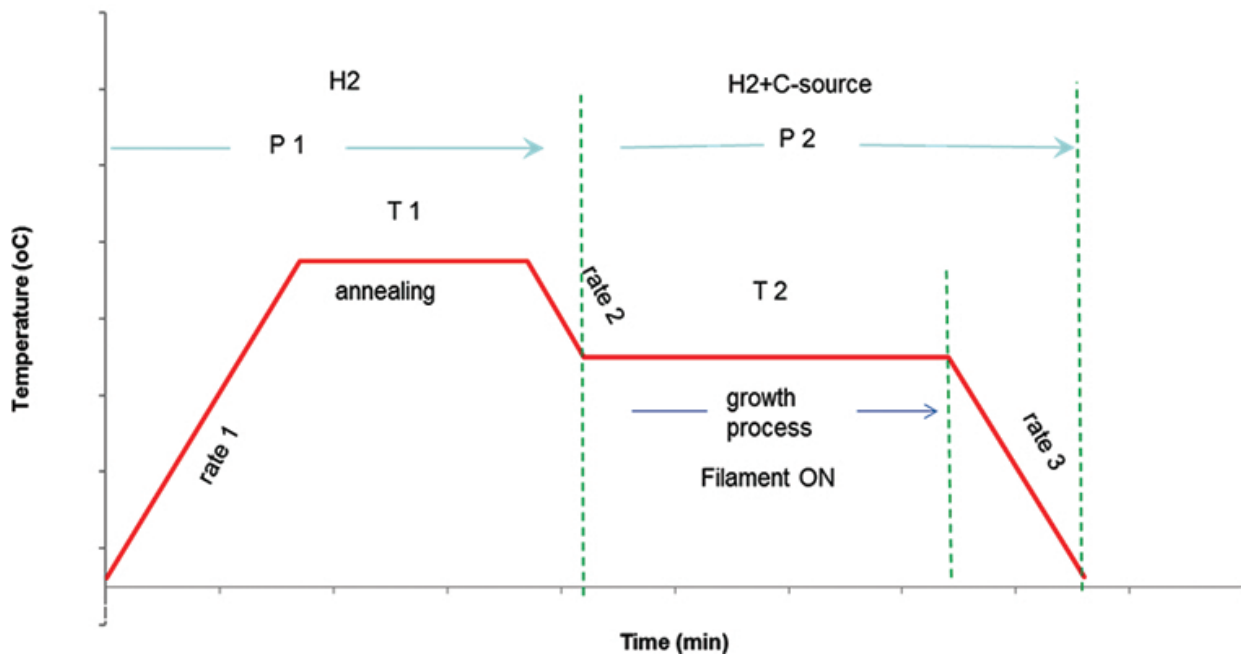


Figure 4. Performance of the temperature during the cleaning process and deposition time.

Mendoza et al. [7] performed a parametric study that included the variation of methane concentration, total pressure, and substrate temperature. The filament-to-substrate distance and filament temperature were kept at 5 mm and 1800°C, respectively. The methane concentration was varied in the 1–50% range in 5% steps, while keeping the pressure at  $4.7 \times 10^3$  Pa and the substrate temperature at 850°C. The ratio of the intensity of the 2D band to that of the G band is used to determine the number of graphene layers, while the ratio of the intensity of the D band to that of the G is used to determine the degree of disorder in the trigonal carbon network.

Graphene growth took place only in the 15–25% methane concentration range. The pressure was then changed in the  $2.7\text{--}4.7 \times 10^3$  Pa range, and the quality of the graphene films deteriorated as indicated by the D band. Increasing the pressure to  $5.3 \times 10^3$  Pa yielded amorphous carbon. The substrate temperature was then lowered from 850 to 750°C in steps of 50°C, resulting in lower graphene quality as indicated by the D band. At temperatures higher than 850°C, the graphene quality improves and monolayer is achieved, but it grows in discontinuous patches. In HFCVD, there seems to be a fundamental trade-off between continuous-discontinuous coverage and bilayer-monolayer graphene [26].

Based on the above-described results, we extended the deposition time from 30 to 100 min for the HFCVD graphene growth in the temperature range from 750 to 1000°C, while keeping the gas mixture of 15% methane in hydrogen at  $4.7 \times 10^3$  Pa. As shown in Figure 5, multilayer graphene is obtained below 850°C, and turbostratic bilayer graphene is obtained between 850 and 1000°C. The most uniform bilayer graphene is obtained at 950°C; the graphene film grown at 1000°C is discontinuous.

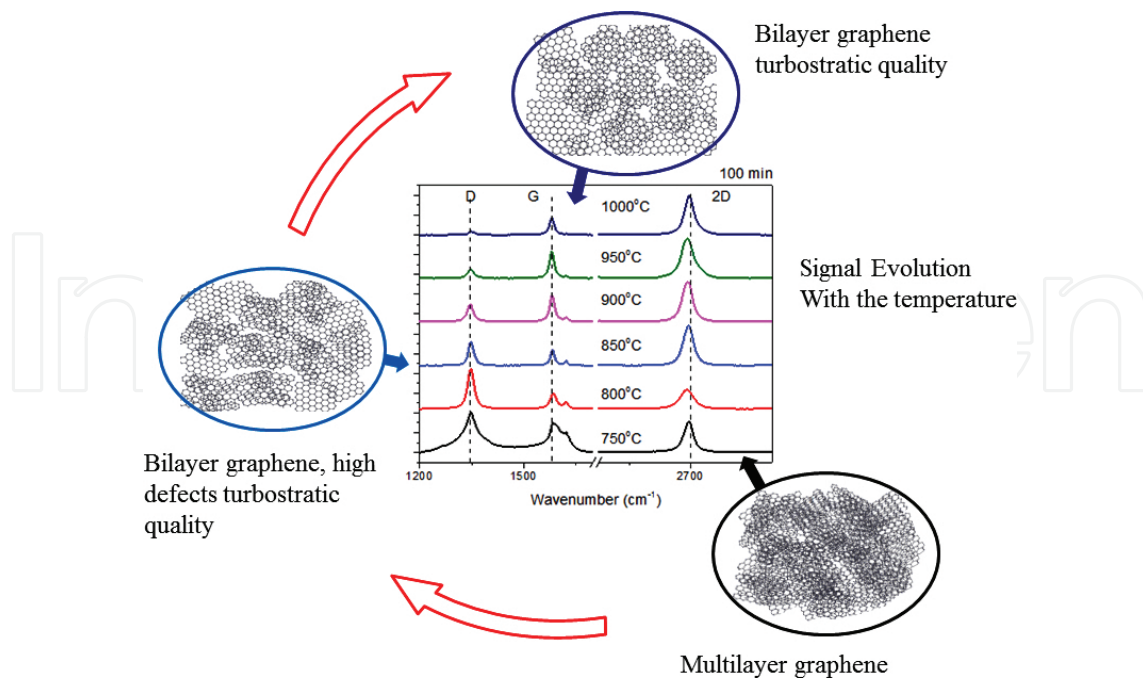


Figure 5. Graphene film evolution as a function of substrate temperature.

We then carried out graphene synthesis experiments as a function of time, keeping the substrate temperature at 950°C and the other parameters constant as well. Figure 6 shows the Raman spectra of the graphene films as a function of deposition time. The optimum bilayer graphene quality and continuous surface is obtained for the 100-min deposition time. As the

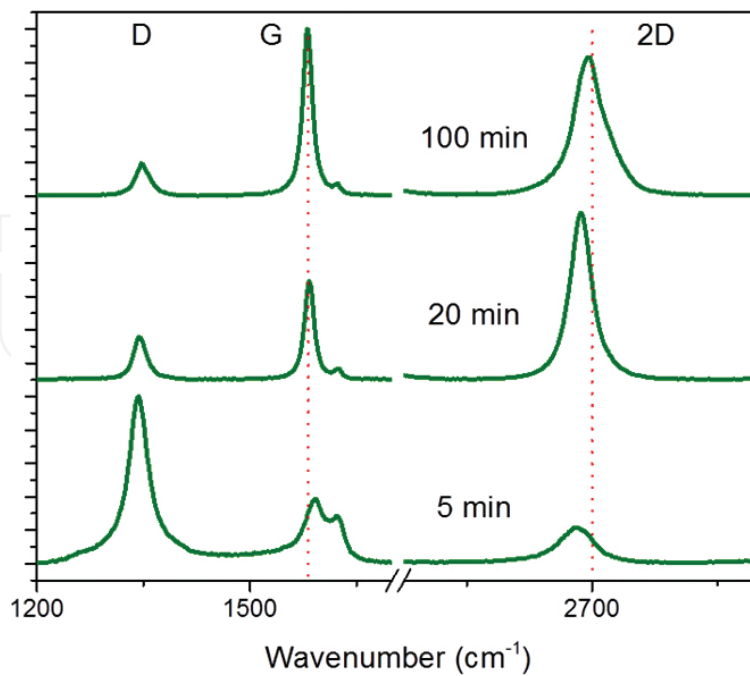


Figure 6. Effect of growth time on bilayer graphene synthesis at 950°C.

deposition time is decreased in 5-min interval down to 20 min, the film continuity is compromised, and gaps remain open on the substrate surface as seen under the optical microscope. The graphene that is grown for less than 10 min shows a very large D band, indicating very small crystallite sizes (<10 nm). Hence, it appears that 100 min allows enough time for the graphene crystallites to grow, defects to heal, and gaps to close. Above 100 min, multilayer graphene starts to dominate the film composition.

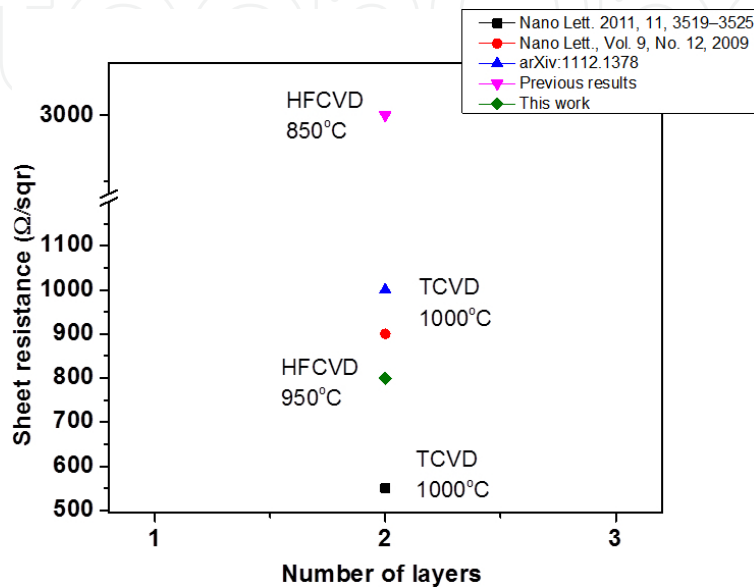


Figure 7. Comparison of sheet resistance values reported for graphene.

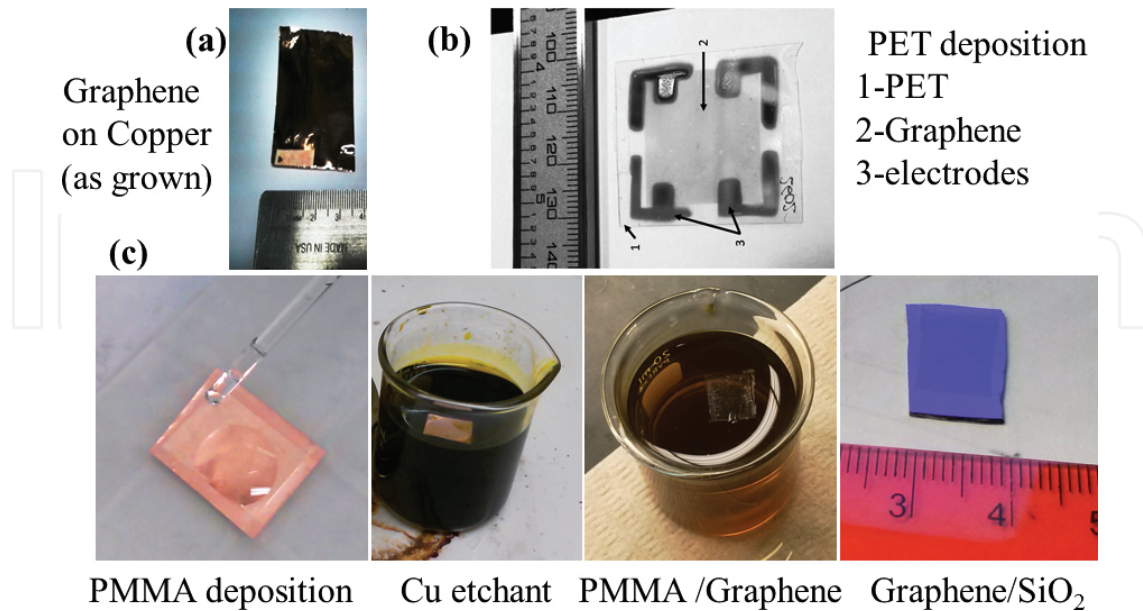


Figure 8. (a) Graphene on copper foil, (b) graphene transferred onto PET, and (c) graphene transfer process from Cu to SiO<sub>2</sub>/Si.

The bilayer graphene grown by HFCVD should also be compared with other graphene reports in terms of transmittance and sheet resistance ( $\Omega/\text{sqr}$ ) [27–31]. **Figure 7** shows the sheet resistance values for HFCVD and hot wall or thermal chemical vapor deposition (TCVD) graphene with visible transmittance in the 90–95% range. The HFCVD bilayer graphene films grown at 850°C show an average sheet resistance in the order of  $3 \times 10^3 \Omega/\text{sqr}$ , whereas those grown at 950°C show an average sheet resistance value in the order of  $8 \times 10^2 \Omega/\text{sqr}$ . The latter value is close to values reported for monolayer graphene grown by TCVD techniques, as seen in **Figure 8**. Moreover, the indium tin oxide (ITO) transparent electrode that is deposited on glass for flat panel systems has sheet resistance values in the order of  $1.5 \times 10^3 \Omega/\text{sqr}$  [32].

## 5. Graphene transfer

For transparent electrode applications, the bilayer graphene grown on copper substrates (**Figure 8a**) must be transferred onto the transparent substrate of choice (e.g., PET, **Figure 8b**). The transfer process is another critical step that can preserve or damage the integrity of the graphene films. First, a polymer support is attached to the graphene film, such as polymethyl methacrylate (PMMA), polydimethylsiloxane (PDMS), polyethylene terephthalate (PET). The polymer support is designed to hold the graphene film when the underlying Cu foil is etched away in iron chloride ( $\text{FeCl}_3$ ) at 70°C, as shown in **Figure 8c**. Once the Cu is removed, the graphene on polymer support is thoroughly cleaned in HCl to remove residual  $\text{FeCl}_3$  and  $\text{Fe}^{3+}$ . Then, the graphene on polymer support is rinsed with deionized water several times and let to dry. The graphene is then ready to be transferred onto any substrate according to the intended application. In the example shown in **Figure 8**, the HFCVD bilayer graphene film was transferred onto a  $\text{SiO}_2/\text{Si}$  wafer by pressing them firmly together and slowly peeling off the polymer support. The integrity of resulting graphene film depends greatly on carefully carrying out the transfer process. The electrical properties of graphene are particularly sensitive to remnant  $\text{FeCl}_3$  impurities and cracks produced in the transfer process.

## 6. HFCVD diamond

Microcrystalline and nanocrystalline diamond films are grown by HFCVD on Si, Mo, and other carbide-forming substrates. The substrates need to be seeded by polishing the surface with  $<0.1\text{-}\mu\text{m}$  synthetic diamond powder. Before the clean reactive gas mixture is introduced into the HFCVD chamber, it is evacuated to  $10^{-3}$  Pa or lower. The gas flow of methane and hydrogen is controlled to obtain fixed methane concentrations of 0.3 and 2.0% for microcrystalline and nanocrystalline diamond, respectively. The gas mixture enters at a rate of 100 sccm and is activated by a heated Re filament positioned at 8 mm above the substrate. The choice of Re for the filament material has the advantage that it does not react with carbon and therefore is not consumed during the diamond reaction. The filament is resistively heated in the range of 2300–2500°C, as measured by an optical pyrometer. The total gas pressure of the chamber is kept at approximately  $2.7 \pm 0.1$  Pa. The substrate temperature can be varied in the 600–900°C range.

The growth rate varies in the 0.1–0.5  $\mu\text{m}/\text{h}$  range depending on the substrate temperature [33]. The SEM images in **Figure 9** illustrate the differences in morphology and grain size between microcrystalline and nanocrystalline diamond.

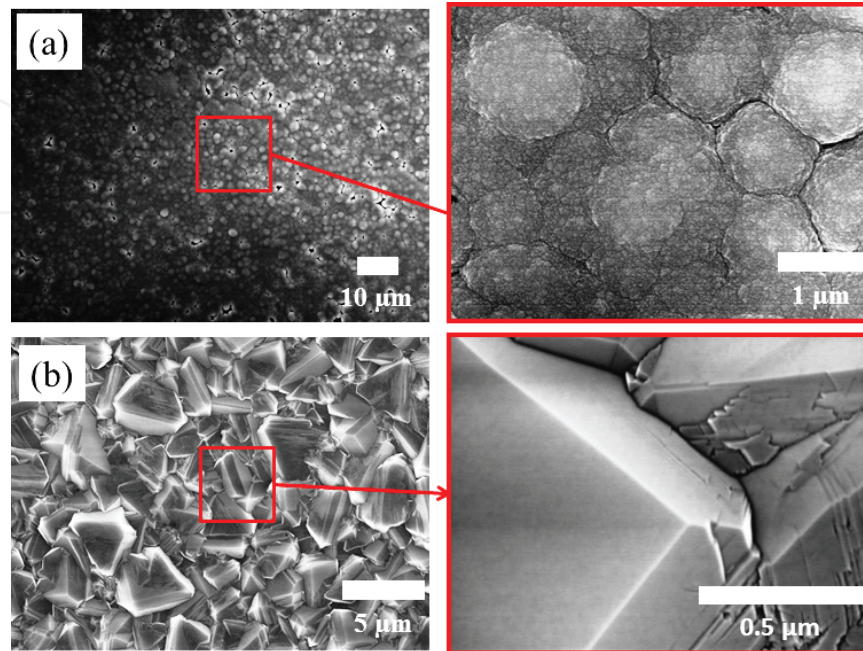


**Figure 9.** Micrographs of (a) nanocrystalline and (b) microcrystalline diamond.

## 7. HFCVD carbon nanotubes

Carbon nanotubes (CNTs) are grown by HFCVD on Cu at a substrate temperature of 900°C using a concentration of 2.0% methane in hydrogen. The growth parameters are similar to those required to grow nanocrystalline diamond; the crucial difference is the choice of substrate material, which should act as catalyst for the growth of CNTs. Before the clean reactive gas mixture is introduced into the HFCVD chamber, it is evacuated to  $10^{-3}$  Pa or lower. The gas mixture enters at a rate of 100 sccm and is activated by a heated Re filament positioned at 8 mm above the substrate. The filament is resistively heated in the range of 2300–2500 °C, as measured by an optical pyrometer. The total gas pressure of the chamber is kept at approximately  $2.7 \pm 0.1$  Pa. A thick layer of carbon nanotubes is readily obtained in about 15 min [34, 35].

The SEM images (**Figure 10a** and **b**) show that the films are composed of entangled clusters of nanotubes or nanofiber structures with the catalyst material present in the form of spherical tips. A more detailed by TEM (**Figure 10c**) shows that the fibers are bamboo-like carbon nanotubes (BCNTs) with diameters ranging from 50–100 nm and variable lengths. They contain nanocavities that are stacked one over the other with closed walls consisting of a number of graphene layers.

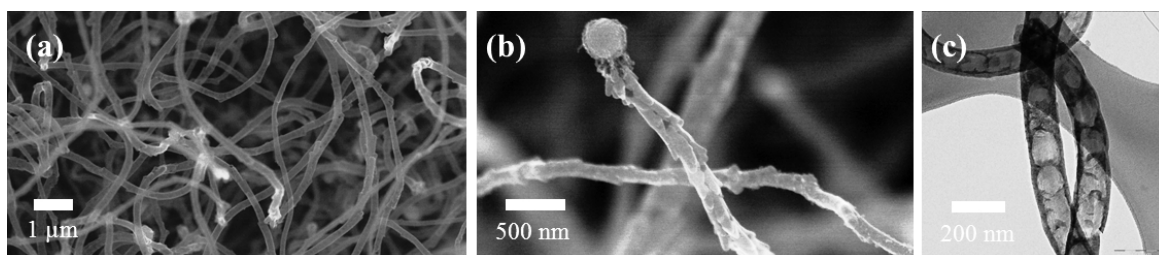


**Figure 10.** Scanning electron microscopy of (a) HFCVD carbon nanotubes, (b) Bamboo-like carbon nanotubes (BCNTs), and (c) transmission electron microscopy of BCNTs.

## 8. Summary

In this chapter, we discussed the HFCVD reactor design and the interplay between the reactor parameters, such as filament and substrate temperatures, filament-to-substrate distance, and total pressure. Special attention was given to the large-area synthesis of bilayer graphene on copper, but we also discussed the HFCVD synthesis of microcrystalline diamond, nanocrystalline diamond, and carbon nanotubes. Large-area bilayer graphene grown by HFCVD has transmittance greater than 90% in the visible region and no gaps. The size of the graphene wafers that can be obtained by HFCVD is only limited by the size of the reactor and lends itself to be incorporated into a continuous roll-to-roll fabrication process, thus lowering the cost per unit area and enabling the integration of bilayer graphene in large-scale industrial production lines. The HFCVD method has the potential to enable large-area applications of graphene, such as transparent electrodes for flat panel displays and solar cells.

## Acknowledgements

This work is funded by the Institute for Functional Nanomaterials (NSF Grant No. 1002410) and in part by PR NASA EPSCoR (NNX15AK43A).

## Author details

Frank Mendoza<sup>1,2\*</sup>, Tej B. Limbu<sup>1,2</sup>, Brad R. Weiner<sup>1,3</sup> and Gerardo Morell<sup>1,2</sup>

\*Address all correspondence to: fran.mendoza@upr.edu

1 Institute for Functional Nanomaterials, University of Puerto Rico, San Juan, USA

2 Department of Physics, University of Puerto Rico at Rio Piedras, San Juan, USA

3 Department of Chemistry, University of Puerto Rico at Rio Piedras, San Juan, USA

## References

- [1] Kusmartsev FV, Wu WM, Pierpoint MP, and Yung KC.; Application of Graphene within Optoelectronic Devices and Transistors. arXiv:1406.0809 [cond-mat.mtrl-sci].
- [2] Novoselov KS, Geim AK, Morozov SV, Jiang D, Zhang Y, Dubonos SV, Grigorieva IV, Firsov AA. Electric Field Effect in Atomically Thin Carbon Films. *Science* 2004;306:666–669
- [3] Park S and Ruoff RS. Chemical methods for the production of graphenes. *Nat. Nanotechnol.* 2009;4:217–224.
- [4] Li X., Cai W., An J., Kim S., Nah J., Yang D., Piner R., Velamakanni A., Jung I., Tutuc E., Banerjee SK, Colombo L and Ruoff RS. Large-area synthesis of High Quality and Uniform Graphene films on Copper Foils. *Science*, 2009, 324, 1312–1314
- [5] Novoselov KS, Fal'ko VI, Colombo L, Gellert PR, Schwab MG, and Kim K. A road map for graphene. *Nature*. 2012;490(7419):192–200.
- [6] Zhang Y, Tsung T-T, Girit C, Hao Z, Martin MC, Zettl A, Crommie MF, Shen YR, and Wang F. Direct observation of widely tunable bandgap in bilayer graphene. *Nature*. 2009;459:820–823.
- [7] Mendoza F, Limbu TB, Weiner BR, and Morell G. Large-area bilayer graphene synthesis in the hot filament chemical vapor deposition reactor. *Diamond Relat. Mater.* 2015;51:34.
- [8] Eigler S, Enzelberger-Heim M, Grimm S, Hofmann P, Kroener W, Geworski A, Dotzer C, Röckert M, Xiao J, Papp C, Lytken O, Steinrück H-P, Müller P, and Hirsch A. Wet chemical synthesis of graphene. *Adv. Mater.* 2013;25:3583–3587.
- [9] Mattevi C, Kim H, and Chhowalla M. J. A review of chemical vapour deposition of graphene on copper. *Mat. Chem.* 2011;21(10): 3324–3334.
- [10] Kim KS, Zhao Y, Jang H, Lee SY, Kim JM, Kim KS, Ahn JH, Kim P, Choi J-Y, and Hong BH. Large-scale pattern growth of graphene films for stretchable transparent electrodes. *Nature*. 2009;457:706–710.
- [11] Li X, Zhu Y, Cai W, Borysiak M, Han B, Chen D, Piner RD, Colombo L, and Ruoff RS. Transfer of Large-Area Graphene Films for High-Performance Transparent Conductive Electrodes. *Nano. Lett.* 2009;9:4359–4363.
- [12] Berger C, Song Z, Li X, Wu X, Brown N, Naud C, Mayou D, Li T, Hass J, Marchenkov AN, Conrad EH, First PN, and Heer WA. Electronic Confinement and Coherence in Patterned Epitaxial Graphene. *Science*. 2006;312:1191–1196.
- [13] Sutter P. Epitaxial Graphene: How silicon leaves the scene. *Nat. Mater.* 2009;8(3):171.

- [14] Wu X, Hu Y, Ruan M, Madiomanana NK, Hankinson J, Sprinkle M, Berger C, and Heer WA. Half integer quantum Hall effect in high mobility single layer epitaxial graphene. *Appl. Phys. Lett.* 2009;95:223108.
- [15] Krupka J and Strupinski W. Measurements of the sheet resistance and conductivity of thin epitaxial graphene and SiC films. *Appl. Phys. Lett.* 2010;96:082101.
- [16] Singh M, Jha HS, and Agarwal P. Growth of Large Sp<sup>2</sup> domain size single and multi-layer graphene films at low substrate temperature using hot filament chemical vapor deposition. *Mat. Lett.* 2014;126:249–252.
- [17] Wiesmann H, Ghosh AK, McMahon T, and Strongin M. J. a-Si:H produced by high-temperature thermal decomposition of silane. *Appl. Phys.* 1979;50:3752.
- [18] Dupuie JL and Gulari E. Hot Filament enhanced chemical vapor deposition of AlN thin films. *Appl. Phys. Lett.* 1991;59(5):549–551.
- [19] Jackson MJ, editor. *Microfabrication and nanofabrication*. Microfabrication and Nanomanufacturing. 1st ed. Boca Raton, FL: International Standard Book. 9780824724313; 2010. 401 p.
- [20] Wei QP, Ashfold MNR, Mankelevich YA, Yu ZM, Liu PZ, and Ma L. Diamond growth on WC-Co substrates by hot filament chemical vapor deposition: Effect of filament-substrate separation. *Diamond Relat. Mater.* 2011;20:641–650.
- [21] Ali M, Ürgen M, and Atta MA. Tantalum carbide films synthesized by hot filament chemical vapor deposition technique. *Surf. Coat. Technol.* 2012;206:2833–2838.
- [22] Kataria S, Patsha A, Dhara S, Tyagi AK, and Barshilia HC. J. Raman, Raman imaging on high-quality graphene grown by hot-filament chemical vapor deposition. *Spectrosc.* 2012;43:1864–1867.
- [23] Behura SK, Mukhopadhyay I, Jani O, Yang Q, and Hirose A. Synthesis and characterization of graphene films by hot filament chemical vapor deposition. *Proceedings of the 24th CANCAM Saskatoon; Saskatchewan, Canada.* 2013.
- [24] Yang Q., Xiao C., Chen W., Singh AK, Asai T., and Hirose A, Growth mechanism and orientation control of well-aligned carbon nanotubes. *Diam. Relat. Mater.* 2003;12:1482–1487.
- [25] Behura SK, Nayak S, Yang Q, Hirose A, Jani O. J. Chemical Vapor Deposited Few-Layer Graphene as an Electron Emitter. *Nanosci. and Nanotechnol.* 2016;16:287–295
- [26] Hawaldar R, Merino P, Correia MR, Bdikin I, Grácio J, Méndez J, Martín-Gago J-A, and Singh MK. Large-area high-throughput synthesis of monolayer graphene sheet by Hot Filament Thermal Chemical Vapor Deposition. *Sci. Rep.* 2012;2:682.
- [27] Chen S, Cai W, Piner RD, Suk JW, Wu Y, Ren Y, Kang J, and Ruoff R. Synthesis and Characterization of Large-Area Graphene and Graphite Films on Commercial Cu-Ni Alloy Foils. *Nano. Lett.* 2011;11:3519–3525.

- [28] Buijnsters JG, Shankar P, van Enckevort WJP, Schermer JJ, and Ter Meulen JJ. The Adhesion of Hot-Filament CVD Diamond Films on AISI Type 316 Austenitic Stainless Steel. *Diamond Relat. Mater.* 2004;13:848–857.
- [29] Chen H, Jang C, Xiao S, Ishigami M, and Fuhrer MS. Intrinsic and extrinsic performance limits of graphene devices on SiO<sub>2</sub>. *Nat. Nanotechnol.* 2008;3:206.
- [30] Li X, Zhu Y, Cai W, Borysiak M, Han B, Chen D, Piner RD, Colombo L, and Ruoff RS. Transfer of large-area graphene films for high-performance transparent conductive electrodes. *Nano. Lett.* 2009;9:124359.
- [31] Lee S, Lee K, Liu C-H, and Zhong Z.; Homogeneous bilayer graphene film based flexible transparent conductor. arXiv:1112.1378 [cond-mat.mes-hall]
- [32] Hong S-J, Kim M-S, Kim J-W, and Shin M. Characteristics of indium-tin-oxide (ITO) glass re-used from old TFT-LCD panel. *Mater. Trans.* 2012;53(5):968–972.
- [33] Gupta S, Weiner BR, and Morell G. J. Synthesis and characterization of sulfur-incorporated microcrystalline diamond and nanocrystalline carbon thin films by hot filament chemical vapor deposition. *Mater. Res.* 2003;18:363.
- [34] Katar SL, Hernandez D, Labiosa AB, Mosquera-Vargas E, Fonseca L, Weiner B, and Morell G. SiN/bamboo like carbon nanotube composite electrodes for lithium ion rechargeable batteries. *Electrochimica Acta* 2010;55:2269.
- [35] Room temperature gas sensor based on tin dioxide-carbon nanotubes composite films. Mendoza F, Hernández DM, Makarov V, Febus E, Weiner BR, Morell G *Sensors and Actuators B: Chemical*; 190:227–233

IntechOpen

